Article

Piezoelectrically and Capacitively Transduced Hybrid MEMS Resonator with Superior RF Performance and Enhanced Parasitic Mitigation by Low-Temperature Batch Fabrication

Adnan Zaman [1], Ugur Guneroglu [2], Abdulrahman Alsolami [1,*] and Jing Wang [2,*]

1 King Abdulaziz City for Science and Technology, Riyadh 12354, Saudi Arabia; azaman@kacst.edu.sa
2 Department of Electrical Engineering, University of South Florida, Tampa, FL 33620, USA; ugur@usf.edu
* Correspondence: aalsolami@kacst.edu.sa (A.A.); jingw@usf.edu (J.W.)

Abstract: This study investigates a hybrid microelectromechanical system (MEMS) acoustic resonator through a hybrid approach to combine capacitive and piezoelectric transduction mechanisms, thus harnessing the advantages of both transducer technologies within a single device. By seamlessly integrating both piezoelectric and capacitive transducers, the newly designed hybrid resonators mitigate the limitations of capacitive and piezoelectric resonators. The unique hybrid configuration holds promise to significantly enhance overall device performance, particularly in terms of quality factor (*Q*-factor), insertion loss, and motional impedance. Moreover, the dual-transduction approach improves the signal-to-noise ratio and reduces feedthrough noise levels at higher frequencies. In this paper, the detailed design, complex fabrication processes, and thorough experimental validation are presented, demonstrating substantial performance enhancement potentials. A hybrid disk resonator with a single side-supporting anchor achieved an outstanding loaded *Q*-factor higher than 28,000 when operating under a capacitive drive and piezoelectric sense configuration. This is comparably higher than the measured *Q*-factor of 7600 for another disk resonator with two side-supporting anchors. The hybrid resonator exhibits a high *Q*-factor at its resonance frequency at 20 MHz, representing 2-fold improvement over the highest reported *Q*-factor for similar MEMS resonators in the literature. Also, the dual-transduction approach resulted in a more than 30 dB improvement in feedthrough suppression for devices with a 500 nm-thick ZnO layer, while hybrid resonators with a thicker piezoelectric layer of 1300 nm realized an even greater feedthrough suppression of more than 50 dB. The hybrid resonator integration strategy discussed offers an innovative solution for current and future advanced RF front-end applications, providing a versatile platform for future innovations in on-chip resonator technology. This work has the potential to lead to advancements in MEMS resonator technology, facilitating some significant improvements in multi-frequency and frequency agile RF applications through the original designs equipped with integrated capacitive and piezoelectric transduction mechanisms. The hybrid design also results in remarkable performance metrics, making it an ideal candidate for integrating next-generation wireless communication devices where size, cost, and energy efficiency are critical.

Keywords: lateral extensional mode; piezoelectric transducers; atomic layer deposition (ALD); thin-film piezoelectric on substrate (TPoS) resonators; microelectromechanical system (MEMS); quality factor

1. Introduction

Radio frequency micro-electro-mechanical systems (RF MEMS) are a transformative technology that has emerged as a key area of research while benefiting from foundry processes. Integrating mechanical and electrical functionalities at a microscopic scale has led to substantial advancements in commercial and military telecommunications, radar, and electronic warfare systems [1]. RF MEMS resonators play a crucial role in various

devices such as oscillators, filters, and frequency synthesizers in RF front ends, where their mechanical vibrations maintain frequency accuracy while ensuring signal integrity in communication systems [2]. Recent advancements in RF piezoelectric arrays have shown that mechanically coupling several identical resonators into an array can effectively reduce the overall motional resistance, despite the trade-off of increased resistance due to reduced transduction areas [3]. Integrating MEMS resonators in consumer electronics and specialized military communication systems has enabled significant device miniaturization and performance enhancement, thus leading to ubiquitous, compact, and high-performance devices essential in our increasingly connected world [4]. The advancements in foundry microfabrication have facilitated the volume manufacturing of devices that perform reliably under varied environmental conditions [5,6].

Capacitively transduced MEMS resonators have been highly valued for their impressive quality factor (*Q*), particularly within the very high frequency (VHF) and ultra-high frequency (UHF) ranges [7]. They operate based on changes in capacitance due to mechanical vibrations in the desired acoustic mode when an electric field aligned with modal vibration is applied, thus enabling them to stabilize resonance frequencies with remarkable timing accuracy. Moreover, the direct integration of capacitively transduced resonators with complementary metal oxide semiconductor (CMOS) transistor circuit technology enhances the microsystem's compactness and functionality. However, capacitive MEMS resonators encounter significant challenges, such as high motional impedance, which complicates their employment with standard 50 Ω RF systems, leading to increased insertion losses [8]. Techniques such as reducing the capacitive transducer air gap all the way down to ~13 nm have been employed to mitigate these issues, although this has caused some problems regarding the force balance of the resonator when a DC bias voltage is applied [9]. On the other hand, piezoelectric RF MEMS resonators, utilizing materials like zinc oxide (ZnO) and aluminum nitride (AlN), are pivotal due to their superb energy conversion efficiency that leads to high electromechanical coupling coefficient [10]. Recent studies have demonstrated that RF piezoelectric arrays, particularly those integrating multiple resonators, effectively reduce motional resistance by leveraging mechanical coupling, which significantly lowers insertion loss and boosts energy conversion efficiency [11]. Furthermore, advances in materials like periodically poled lithium niobate and contour-mode aluminum nitride, along with optimized electrode designs, have significantly improved the quality and performance of piezoelectric resonators across a broad frequency range [12]. With strong electromechanical coupling coefficients, these materials enable piezoelectric resonators to operate with lower motional impedance and improved insertion loss characteristics as compared to their capacitive counterparts. Meanwhile, piezoelectric resonators encounter their own challenges, such as thermal budget constraints set by post-CMOS fabrication processes, often necessitating high processing temperatures incompatible with integrated circuit technologies. Also, resonators with piezoelectric transducers are often more susceptible to excitation of spurious modes, which has imposed significant challenges and device-specific solutions [13–15]. By fully leveraging the benefits of both capacitive and piezoelectric transducers, RF MEMS resonators have the potential to revolutionize the field while fueling new applications [16].

2. Background and Motivation

The development of RF MEMS technology is critical to advancing global telecommunications infrastructure and defense capabilities. Hence, the integration of capacitive and piezoelectric transduction mechanisms within a single hybrid MEMS resonator represents a potential technological leap forward. This is due to the need to overcome the inherent limitations of single-transduction systems in terms of frequency agility, port-to-port isolation, susceptibility to spurious modes, power efficiency, and miniaturization. The hybrid MEMS resonators combine the high-quality factors and low spurious mode susceptibility of capacitive transduction with the low insertion loss (strong electromechanical coupling

coefficients) of the piezoelectric one, thus holding the potential to improve the overall device performance.

Moreover, the Internet of things (IoT), ubiquitous wireless sensors, and smart city devices require sophisticated communication protocols, which underscore the growing importance of on-chip MEMS technologies in providing critical solutions for intelligent, ubiquitous, and low-power applications [17]. This work aims to position hybrid MEMS resonators as central components in future RF systems by offering an alternative solution to the current technologies, including both capacitive and piezoelectric resonators, which benefits from its unique ability to seamlessly consolidate the advantages of two transducer technologies into one standalone resonator. In particular, we focus on addressing the issue of parasitic feedthrough, which is a key challenge in MEMS resonators. Feedthrough suppression is crucial since it allows the desired resonance signal to be detected easily from the background noise. Both capacitive and piezoelectric resonators have employed various techniques to decrease feedthrough levels in prior works, such as differential measurement techniques [18], dummy twin designs [19], and the use of peripheral electrodes [20]. However, these methods often require additional complexity in device structure, circuit-level trick, fabrication technique, and measurement scheme.

Conversely, the hybrid resonator device studied in this work, which operates on a two-port scheme, inherently exhibits low feedthrough levels without imposing additional design complexity. This makes our device not only competitive in terms of feedthrough levels to all prior works, but also potentially desirable in terms of simplicity and effectiveness when compared to existing technologies. Also, this low-feedthrough characteristic makes the proposed device configuration well suited as a sensing element in applications like MEMS gyroscopes [21] and local oscillators with a MEMS tank circuit [22], where high feedthrough can be detrimental from a signal-to-noise ratio perspective. The hybrid MEMS resonator scheme achieves low feedthrough levels inherently, thus offering a streamlined solution for low-parasitic operation, while retaining the overall performance. This innovation holds exceptional promises for microsystem applications, where feedthrough mitigation is crucial for key device functionality. It is anticipated that these devices hold unique abilities to offer superior performance with enhanced frequency control and stability, better noise characteristics, and greater efficiency. Ultimately, this could lead to more reliable and robust RF front-end systems [1,2,4,7–10,16], while enabling emerging applications in wearable technology, flexible electronics, and advanced sensor networks [23–27]. The newly investigated hybrid resonator configuration could pave the way for MEMS resonator technologies to evolve and meet the increasingly stringent demands of modern and future wireless communication technological landscapes.

3. Device Structure and Operation

Hybrid MEMS resonators are configured from a novel concept to integrate capacitive and piezoelectric transduction mechanisms for activation and sensing of the target modal resonance. The main design strategy aims to achieve superior performance metrics, almost double the Q-factor value reported in literature as illustrated in Table 1, by leveraging the distinct advantages of each transduction mechanism within a single device. Specifically, hybrid resonators address the limitations of each standalone system, thereby enhancing overall device performance, including quality factor (Q), insertion loss, and motional impedance. The high Q, low power consumption, and low spurious mode susceptibility of capacitive resonators could be combined with the low motional impedance and robust frequency control of piezoelectric resonators, promising more flexible frequency tuning and improved thermal stability.

Hybrid resonators are typically composed of micromachined silicon resonator body structures that incorporate both capacitive and piezoelectric transducers. The design often involves a layered approach, where a piezoelectric thin film (e.g., ZnO or AlN) is deposited onto a pre-fabricated capacitive resonator body microstructure composed of silicon or another semiconductor material such as diamond, silicon carbide, or fused silica.

Table 1. Comparison of the performance metrics of various MEMS resonators, including devices with capacitive, piezoelectric, and hybrid (capacitive/piezoelectric) transduction mechanisms.

Reference	Transduction Mechanism	Frequency (Hz)	Bias Voltage (V)	Gap Width (nm)	Q	R_m (Ohm)
[28]	Capacitive	9.65×10^7	7	100	3600	1.75×10^4
[29]	Capacitive	3.4×10^4	2.5	1000	60,000	4×10^4
[30]	Capacitive	1.07×10^8	N.A.	70	12,400	1.13×10^6
[31]	Capacitive	2.27×10^6	3.6	159	1000	3.95×10^5
[32]	Capacitive	51.33×10^6	4	70	8200	1.778×10^6 (*)
[33]	Piezoelectric	132.94×10^6	N.A.	N.A.	1099	246
[34]	Piezoelectric	4.96×10^8	N.A.	N.A.	3800	600
[35]	Piezoelectric	1.97×10^9	N.A.	N.A.	3410	340
[36]	Piezoelectric	8.82×10^8	N.A.	N.A.	220	98.76
[37]	Hybrid	101.65×10^6	20	150	14,000	2.411×10^3 (*)
[38]	Hybrid	14.63×10^6	~70–141	2500	1952	1.2×10^3
[39]	Hybrid	167×10^6	N.A.	200	4536	4.94×10^3
This Work	Hybrid	20×10^6	12	84	28,677	199.43×10^3

* Calculated from the [37] based on reported insertion loss by using equations in [40].

This unique multi-layer configuration allows for the efficient coupling of mechanical and electrical energy while maximizing the resonator's performance. The piezoelectric layer is activated by electrical signals that induce mechanical strains, thereby generating an electric field across the material. On the other hand, the capacitive transducer component generates an output motional current signal by sourcing it from the changes in capacitance caused by mechanical modal vibrations. A key challenge in designing hybrid resonators is the need to integrate different material systems with distinct physical properties and processing requirements. For example, the high-temperature processes required for piezoelectric materials can affect the structural integrity of the capacitive components. To tackle this challenge, it is crucial to develop innovative and robust fabrication techniques that can effectively incorporate these materials while maintaining optimal device performance. The detailed design of hybrid MEMS resonators that seamlessly integrate capacitive and piezoelectric transduction mechanisms to enhance performance metrics such as quality factor, insertion loss, and motional impedance, and so on, is depicted in Figure 1.

Addressing parasitic effects that arise from the close proximity of capacitive and piezoelectric transducer elements is crucial. Strategies such as optimizing electrode placement and employing advanced materials that minimize electrical crosstalk and mechanical losses were used to enhance the resonator's performance. The resonator's design, such as layer thicknesses and lateral sizes and electrode designs, are adjusted to determine its resonance frequency and electromechanical coupling coefficient directly.

By employing a one side-supporting anchor with strategically designed dimensions, acoustic energy losses through the anchor have been effectively minimized. To excite wine-glass mode while reducing anchor-related losses, the supporting tethers should be placed at quasi-nodal locations where the resonator plate has no radial displacement. In this work, resonator designs with both one and two side-supporting anchors were used, among which the design with one anchor showed better performance. Single-anchor designs generally exhibit higher quality factors and reduced energy losses compared to double-side-supporting anchor designs due to less energy dissipation through the support structure [28]. The COMSOL® finite element eigenfrequency simulation, as shown in Figure 2, depicts the first four lateral extensional contour modes of a disk resonator.
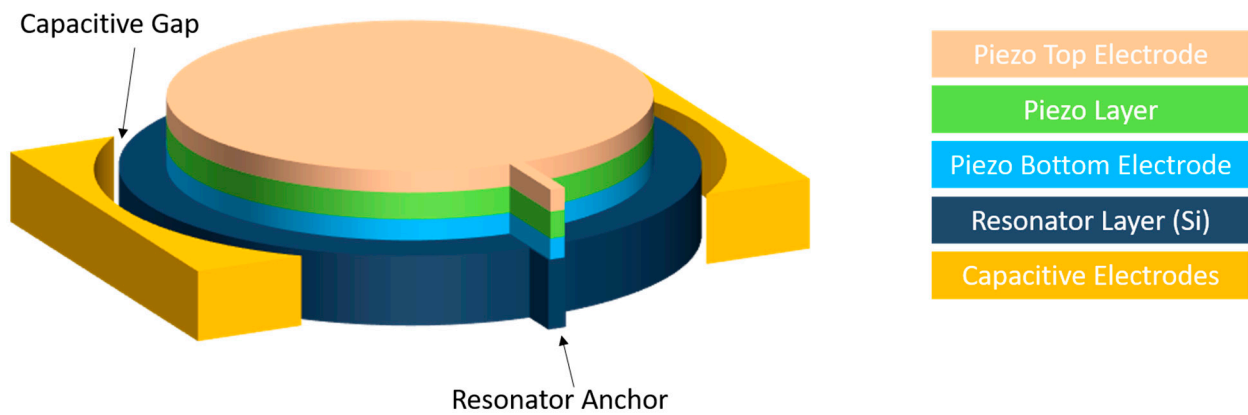
Figure 1. Schematic illustration of electrode and anchor design configurations for a hybrid MEMS resonator. This hybrid resonator integrates capacitive and piezoelectric transducers, which are designed to enhance performance metrics such as quality factor, insertion loss, and motional impedance, and so on.
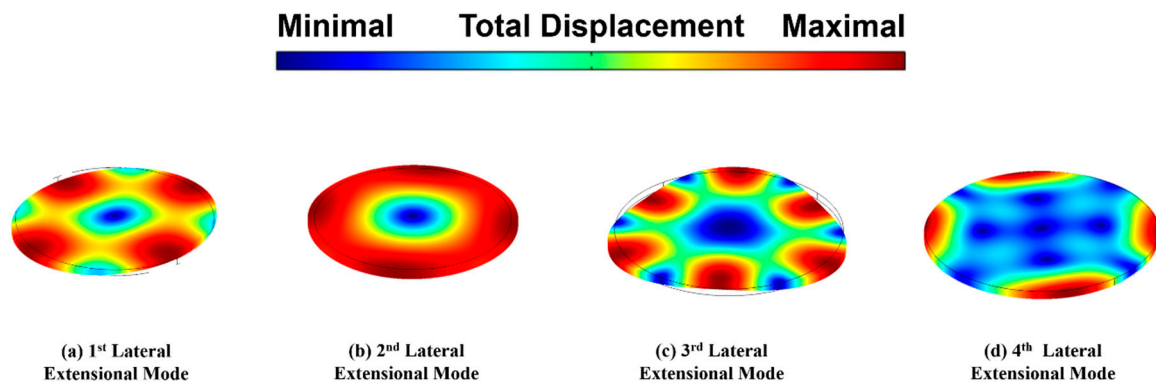

Figure 2. COMSOL® finite element eigenfrequency simulation depicting the first four lateral extensional contour modes of a disk-shaped resonator: (**a**) 1st lateral extensional mode, (**b**) 2nd lateral extensional mode, (**c**) 3rd lateral extensional mode, (**d**) 4th lateral extensional mode.

4. Fabrication Process

The hybrid MEMS resonator microfabrication process is a complex endeavor that integrates both capacitive and piezoelectric transducers to implement a lateral–extensional mode resonator with potentials for superior RF performance characteristics. Figure 3 depicts the fabrication process of the capacitive and piezoelectric hybrid resonator. A silicon-on insulator (SOI) wafer with a 500 μm Si substrate layer, a 2 μm buried oxide layer, and a 10 μm silicon device layer has been used as the starting substrate, as seen in Figure 3a. Each step in the process flow is crucial to ensure the optimal performance and reliability of fabricated hybrid resonators. The process begins with the fabrication of a capacitively transduced resonator, where a silicon substrate is coated with a five μm-thick layer of AZ12xt photoresist that has been selected due to its resistance to dry-etching processes [26,33]. This is followed by meticulous etching using a modified high-aspect ratio deep-reactive ion-etching (HAR DRIE) Bosch recipe to define the microstructural framework that is necessary for the capacitive elements of the resonator. After the etching, a critical 80–90 nm-thick gap spacing layer of Al_2O_3 is deposited through atomic layer deposition (ALD), which serves to define the precise capacitive air gaps essential for the capacitive resonator's functionality, such as the electromechanical coupling coefficient. To enhance the structural integrity and performance, the capacitive electrodes are anchored directly to the SOI silicon substrate layer rather than just being positioned atop the gap spacing layer. This modification is achieved by selectively etching the ALD gap spacing layer from the sidewalls of the capacitive electrodes, using a combination of special masking

and a 6:1 buffer oxide etch (BOE). This step ensures the surrounding capacitive electrodes are attached to the SOI silicon substrate layer, preventing delamination during subsequent fabrication processes.
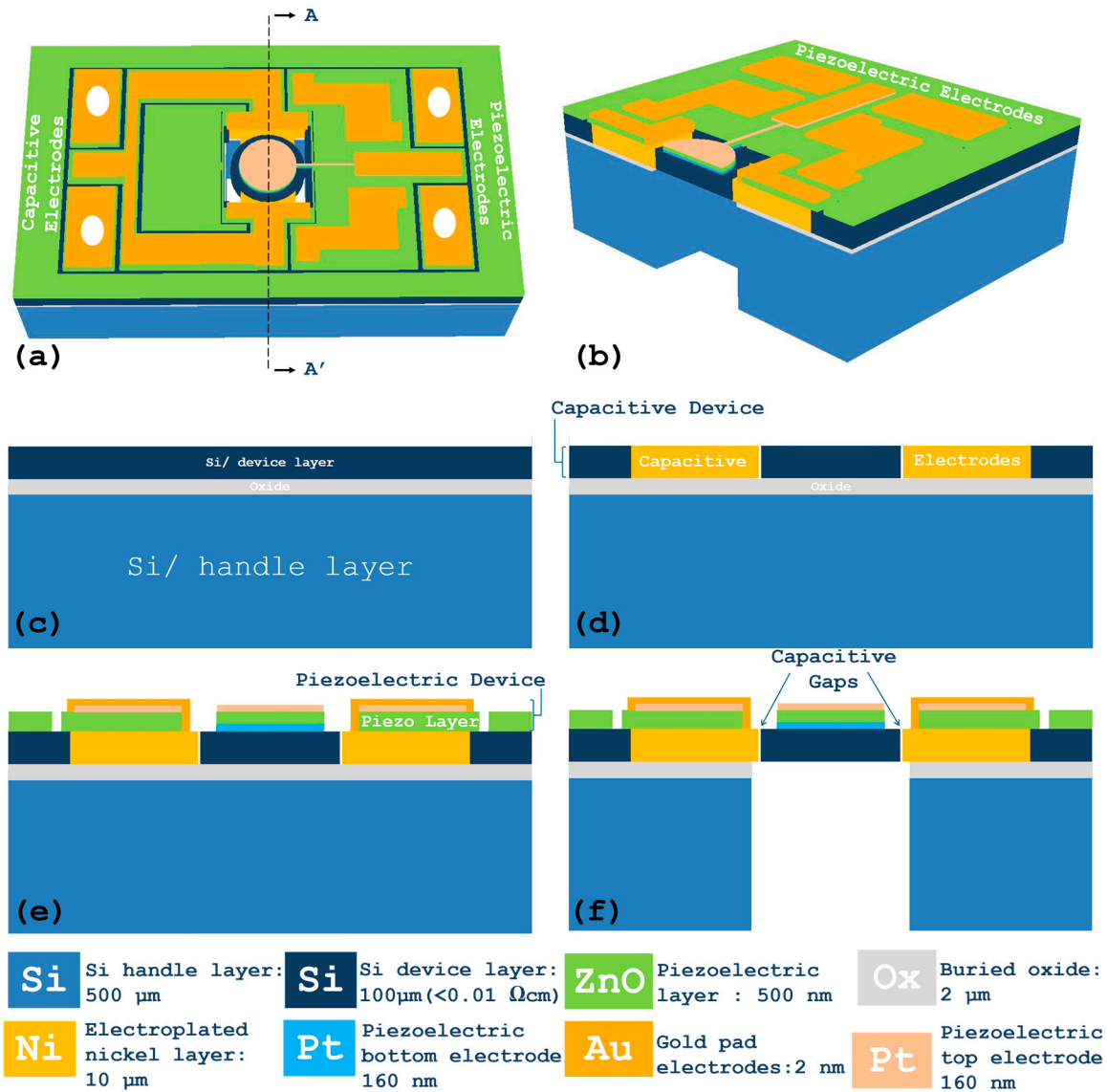

Figure 3. (**a**) Top-view (3D) and (**b**) cross-sectional view (3D) diagrams of proposed hybrid resonator; (**c**–**f**) step-by-step illustration of the simplified fabrication process flow of a hybrid lateral extensional mode resonator with capacitive and piezoelectric transducers. The process begins with the preparation of a silicon-on-insulator (SOI) wafer and proceeds through steps such as photolithography, deep-reactive ion-etching (DRIE), atomic layer deposition (ALD) for gap spacing, and the deposition of a ZnO piezoelectric layer, which concludes with the final releasing step to suspend the resonator structure.

Following the structural modifications, a seed layer made of a chrome adhesion layer and a copper layer is deposited by sputtering for the electroplating of capacitive electrodes. Nickel electroplating is then employed to form the thick capacitive electrodes that enclose the resonator body. This involves a detailed lithography step to define a mold for plating over selective areas within a thick layer of photoresist, ensuring precise deposition of nickel to form patterned surrounding capacitive electrodes. The activation of the seed layer prior to electroplating is critical and involves treating the wafer in a solution of ammonium hydroxide to remove any oxide that could impede the plating

process. Before the piezoelectric layer is deposited, the wafer undergoes a planarization process via chemical–mechanical polishing (CMP) to ensure a uniform top surface across all structures by thinning them down to 5 μm. CMP process ensures devices modal vibration functionality at the targeted resonance. In addition, due to the CMP's high-precision process and fabrication tolerance, the employment of the CMP step ensures the reliability and repeatability of the measured devices. Similar to transistor foundry processes, this CMP planarization is also crucial for the subsequent deposition and patterning of the piezoelectric material, as shown in Figure 3b. The RF magnetron sputtering of the piezoelectric ZnO layer is critical for the fabrication of piezoelectric resonators, particularly due to the strong correlation between the degree of c-axis orientation and the value of the d_{31} transverse piezoelectric coefficient. Achieving a high transverse piezoelectric coefficient d_{31} is essential for optimizing the performance of ZnO resonators, necessitating the deposition of high-quality (002) c-axis-oriented ZnO thin films with densely packed columnar structures. The process begins with the RF sputtering of ZnO onto the resonator body structure, which includes a conductive bottom electrode. For piezoelectrically transduced contour-mode resonators and filters, where in-plane extensional motions are critical, the quality of the ZnO films is vital. These films must exhibit strong c-axis orientation to convert electrical signals into mechanical vibrations and realize a high electromechanical coupling coefficient.

The substrate temperature during deposition plays a crucial role in the piezoelectric properties of the ZnO films. The optimal results were observed at a substrate temperature of 300 °C [26,33,40], under which the ZnO film demonstrated the highest intensity peak of c-axis orientation. This condition leads to better piezoelectric characteristics compared to films deposited at higher or lower temperatures, where the quality and dielectric properties degrade. Maintaining an optimal substrate temperature ensures that the 500 nm-thick ZnO films are deposited under conditions that favor the growth of piezoelectrically active phases with solid electromechanical coupling coefficients. The oxygen environment during sputtering is essential for ensuring an oxygen-rich ZnO film. It is crucial to maintain a balanced argon–oxygen ($Ar:O_2$) gas flow ratio; our experiments have shown that a 1:1 ratio promotes the strongest (002) crystalline orientation. Deviations in this ratio can significantly affect the film's quality. An increase in oxygen ratio can lead to degradation, while a decrease can negatively impact the dielectric effect and increase the conductivity of the film. The precise control of the oxygen environment during the deposition process is vital for achieving the desired electrical and mechanical properties of the ZnO layer.

Following deposition, the ZnO film undergoes an annealing process at 400 °C for one hour under a forming gas environment with Ar and O_2. This post-deposition treatment is vital for enhancing the piezoelectric crystal characteristics and improving the c-axis alignment. The annealing process helps to relieve internal stresses in the film and promotes the reorientation of piezoelectric crystal domains, which enhances the material's piezoelectric coefficient. The exploration of deposition conditions, from the sputtering environment to the post-deposition annealing, optimizes the ZnO's piezoelectric properties, thus ensuring that the final hybrid resonators meet the stringent demands of advanced RF applications. Each process parameter is tuned to optimize the resonator's response, proving essential for achieving high performance and reliability for advanced RF MEMS devices.

After the sputter deposition of ZnO film under optimized process conditions, the next crucial step is the selective wet etching of the Al_2O_3 sacrificial gap layer. This clears the way for the subsequent stages that resemble piezoelectric resonator fabrication. The ZnO layer is subsequently etched by diluted hydrochloric acid to pattern the via-holes, which are carefully engineered to expose the bottom electrode without compromising the integrity of the piezoelectric material. The top electrode is then deposited and patterned by the lift-off method, finalizing the electrical contacts necessary for device operation under desired excitation signals. To ensure that each functional block of the resonator operates independently without strong interference, a deep-reactive ion-etching (DRIE) is employed, as seen in Figure 4. This step is critical, as it not only defines the resonator body but also

establishes clear isolation between ports and the ground, thus maintaining the resonator's performance under various operational conditions, as illustrated in Figure 3e.
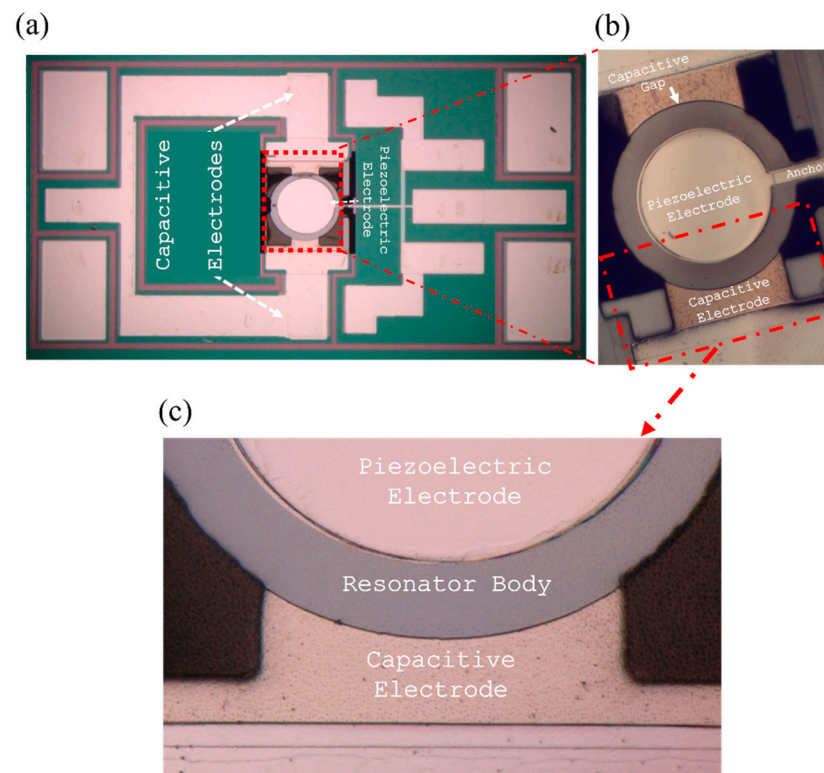

Figure 4. (**a**) Top-view microscope image of the fabricated hybrid resonator after etching the ZnO piezoelectric transducer and silicon device layer to define the disk resonator body, (**b**) Zoomed-in view of the device showing piezoelectric and capacitive transducers. (**c**) Further zoomed-in view photo showing the resonator body with piezoelectric and capacitive electrodes, and the capacitive air gap between the resonator body and the capacitive electrode.

The final fabrication step of the hybrid resonator is to release the resonator structure, which is achieved through a process of backside wafer etching, as shown in Figure 3f. This critical phase involves selectively etching away the underlying layers from the back of the wafer, effectively suspending the resonator structure on the front side of the substrate. This suspension is essential for ensuring that the resonator is completely rereleased, minimizing any potential substrate coupling and feedthrough interactions that could negatively impact the device's performance. The precision and repeatability of the rear side release etching process are crucial as they not only enable the resonator to perform optimally under its lateral extensional mode but also safeguard its structural integrity.

The fabrication exploits the intricate and precise nature of foundry-compatible manufacturing of hybrid MEMS resonators. Each step, from the first photolithography to the final rear side dry-etching release, plays a pivotal role in achieving the desired performance characteristics and high yield, enabling these resonators to perform effectively in advanced RF front-end applications. Figure 4 presents microscope image of the fabricated hybrid resonator.

5. Parasitic Effects and Compensation Techniques

A typical MEMS resonator that is fabricated on SOI substrate has parasitic effects that limit the performance (e.g., the port-to-port isolation) of a capacitive or piezoelectric micromechanical resonator. The imperfect ground shielding provided by the SOI wafer's silicon handle layer contributes to a capacitive feedthrough signal between the drive and sense electrodes, which increases the port-to-port feedthrough noise floor to such an extent

that the resonance peaks of the resonator device layer are often strongly distorted by the parasitic feedthrough noise floor. These parasitic effects demand special compensation.

Figure 5 illustrates the feedthrough signal paths for both capacitive and piezoelectric resonators. The air gap in the capacitive resonator limits the RF signal path of the feedthrough signal to traveling primarily through the SOI substrate under each device. Since the capacitive air gap provides superior signal isolation than that of piezoelectric thin film with higher capacitive coupling between piezoelectric electrodes, the overall parasitic feedthrough signal is considerably lower for resonators equipped with capacitive air-gap transducers, since the RF feedthrough signal predominantly travels between the actuation and sensing electrodes through the SOI wafer handle layer (i.e., the silicon layer underneath the buried oxide layer). Conversely, piezoelectric resonators heavily rely on the two closely positioned input and output electrodes that sit next to each other on top of the piezoelectric transducer thin film for actuation. Thus, the RF feedthrough signal can travel through the SOI substrate and the piezoelectric transducer layer. Additionally, Figure 6 presents the equivalent circuit models within an SOI wafer for both capacitively and piezoelectrically transduced resonators, while depicting inductance–capacitance–resistance (LCR) circuit components in the form of Butterworth–Van Dyke (BVD) model for the resonator as well as the key parasitic elements between electrodes and through the substrate.
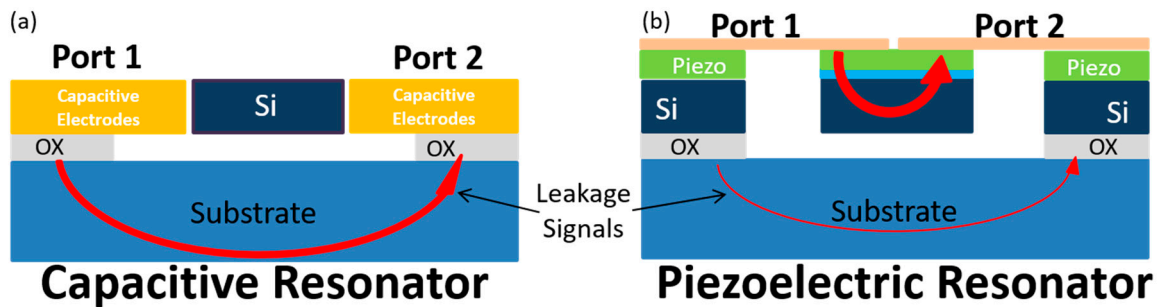

Figure 5. Conceptual illustration of the primary feedthrough signal paths with different strengths for (**a**) a capacitively transduced resonator, and (**b**) a piezoelectrically transduced resonator.
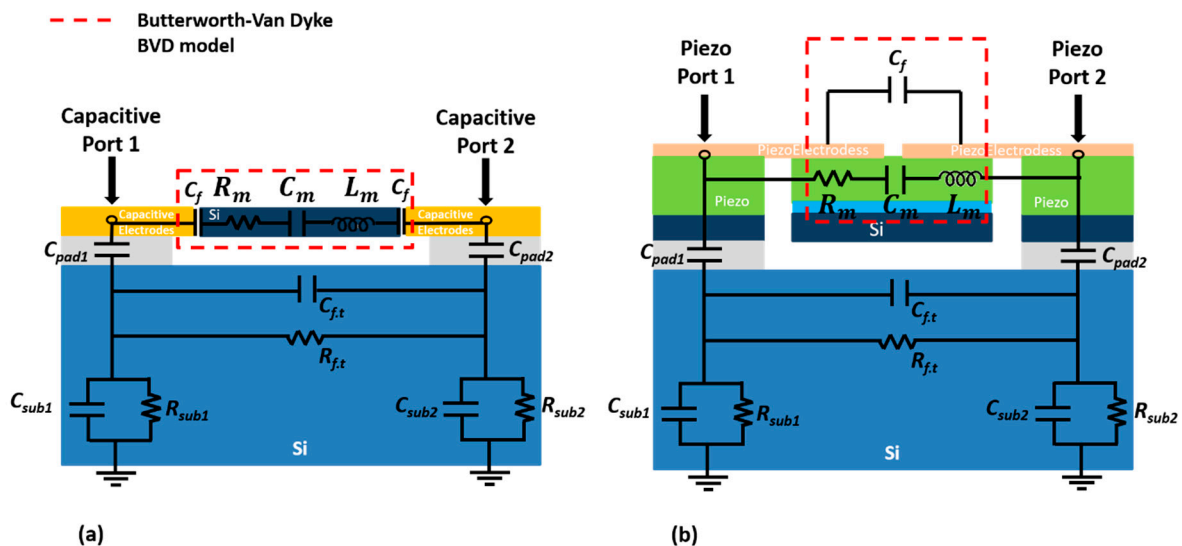

Figure 6. Cross-sectional schematic of a resonator device fabricated in an SOI wafer depicting the LCR circuit components, showing the key parasitics between electrodes and through the substrate, for (**a**) a capacitively transduced resonator, and (**b**) a piezoelectrically transduced resonator.

The hybrid MEMS resonator design herein significantly mitigates parasitic effects by leveraging the distinct advantages of both capacitive and piezoelectric transduction mechanisms. The design strategically integrates these mechanisms to reduce both parasitic

capacitance and acoustic modal coupling, which are prevalent in standalone systems. By physically isolating the capacitive and piezoelectric transducers, inserting an interlayer ground plane as the bottom electrode of the piezoelectric transducer, and optimizing the capacitive and piezoelectric electrode placements, the hybrid resonator design mitigates the direct electrical feedthrough paths that often lead to unwanted capacitive coupling. This isolation is enhanced by employing advanced materials and fabrication techniques that inherently limit electrical crosstalk and mechanical acoustic modal interference.

Figure 7 depicts the strategic combination of transduction mechanisms in hybrid resonators, which significantly enhances the signal-to-noise ratio by fully leveraging the individual strengths of both capacitive and piezoelectric transducers. As shown in Figure 7a, by employing two piezoelectric electrodes (ports 3 and 4) for actuation and two capacitive electrodes (ports 1 and 2) for sensing, this design scheme not only minimizes cross-talk between input and output ports but also enhances the suppression of spurious modes. This hybrid configuration promotes a cleaner resonance signal response, as capacitive transducers are particularly effective in selectively detecting the response of the targeted resonance mode in a spurious-mode free fashion. Conversely, Figure 7b illustrates another operation scheme by this exact hybrid resonator, where the two capacitive electrodes are used for actuation, and the two piezoelectric electrodes are employed for sensing (detection of the resonance response). This setup further isolates the input signal from the output signal as the capacitive transducers surrounding the resonator body are shielded from the piezoelectric transducer electrodes that are separated by the ground electrode and piezoelectric transducer film in between two kind of transducer electrodes, thereby reducing cross-talk and leveraging the distinct isolation properties of the piezoelectric transducer components (ground shielding).
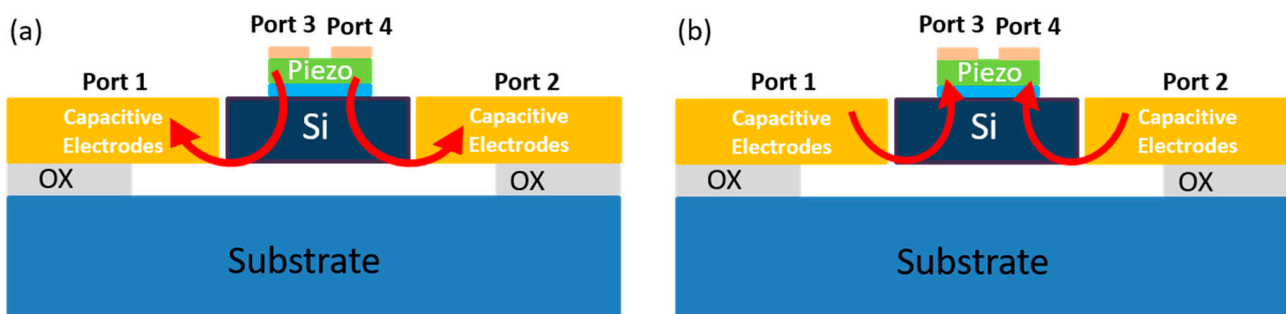
Figure 7. Illustration of signal paths for a hybrid capacitive/piezoelectric resonator with reduced feedthrough as the device operates under different configurations, including (**a**) piezoelectric drive and capacitive sense, and (**b**) capacitive drive and piezoelectric sense.

6. Experimental Results

Hybrid MEMS resonator devices have been characterized by on-wafer probing using an RF probe station under normal atmospheric pressure and ambient temperature. The RF probe testing utilized a CS−5 Short-Open-Load-Thru calibration standard kit from GGB Industries Inc., ensuring accurate de-embedding to bring the reference planes to the end of the probe tips. It was observed that some hybrid resonator devices experienced electrical short-circuiting at low bias voltages, which indicates particle intrusion into air gaps between surrounding capacitive electrodes and the resonator body, a common issue when drying MEMS devices with solvents under atmospheric pressure. To circumvent this issue and prevent capillary forces from drawing particles into these capacitive gaps, a critical CO_2 drying system is advised immediately after the HF or buffered oxide etch (BOE) wet-etching process for gap spacing oxide removal to avoid potential microfabrication complications, especially for small gap sizes, including stiction [9,28,33].

Figure 8 shows a top-view SEM photo of a fabricated hybrid disk resonator, which consists of dual capacitive electrodes enclosing the resonator body to form a pair of lower-layer capacitive ports, with one or a pair of electrodes atop the piezoelectric layer above the disk-shaped resonator body functioning as one or two additional piezoelectric transducer ports. A versatile two-port measurement setup using a vector network analyzer (VNA) and a power supply were employed to evaluate the S-parameter frequency responses and investigate the quality factor and resonance frequency. The hybrid resonator device has been tested under two distinct measurement schemes: one that applies DC bias directly to the piezoelectric bottom electrodes, isolating the ground plane completely; and another that uses a bias tee to apply both AC and DC voltages to the capacitive electrodes, with the motional current detected from the top-layer piezoelectric electrode, as shown in Figure 8.
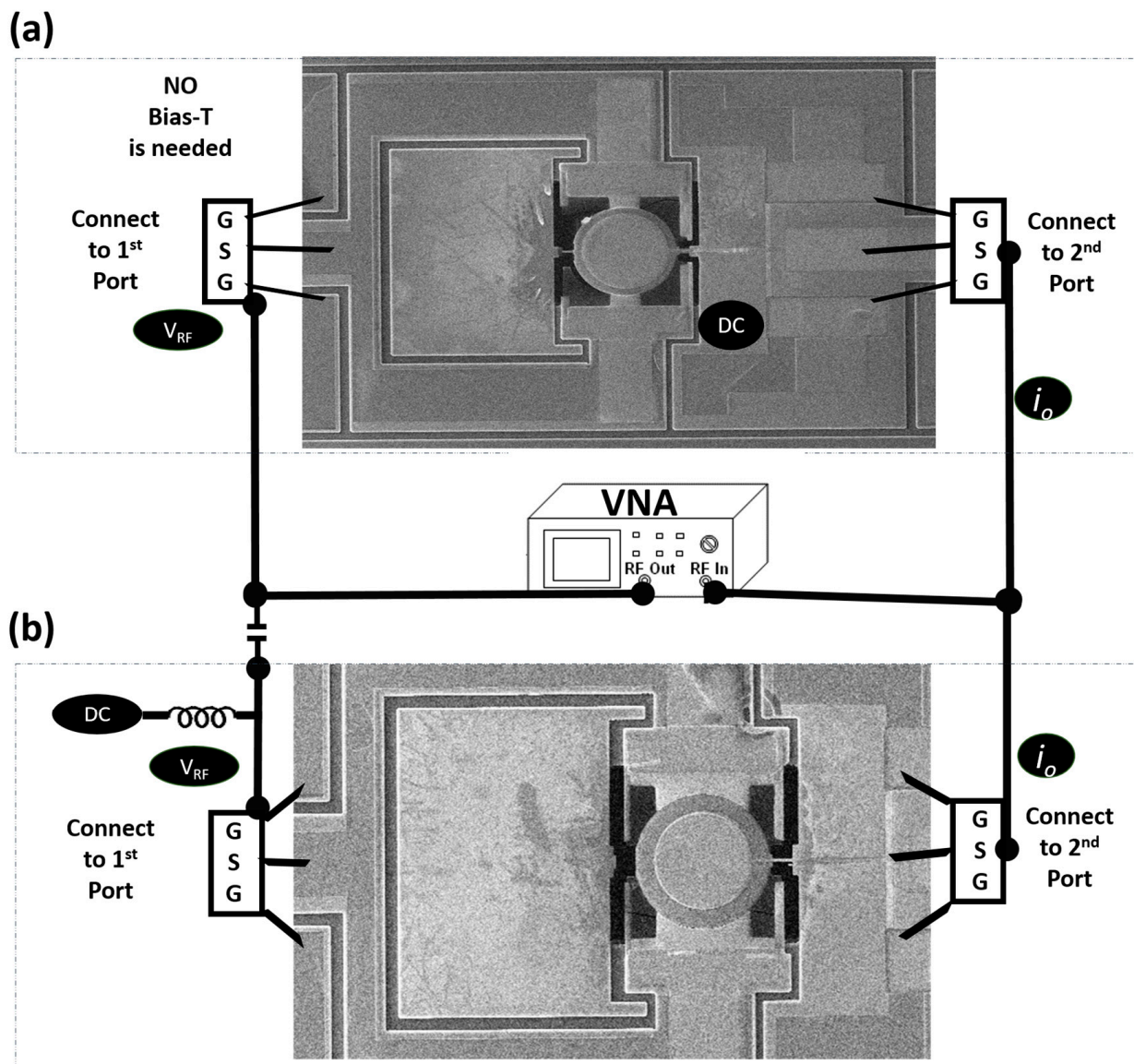

Figure 8. Illustration of RF probe measurement set-up for hybrid resonator devices with a set of two capacitive ports and another one or a pair of piezoelectric transducer ports, fully isolated by the resonator body and ground, showing two different activation schemes to generate electrostatic force in the capacitive gap. (**a**) One applies an AC voltage to the capacitive electrodes and a DC voltage to the resonator body with two anchors to generate electrostatic force; and (**b**) The other applies both AC and DC voltages to the capacitive electrodes to induce electrostatic force in the capacitive gap for a resonator design with wider capacitive electrodes and one side-supporting anchor.

Furthermore, feedthrough signal level measurements have been conducted, which are crucial for quantifying parasitic effects for limiting high-frequency port-to-port isolation within piezoelectric, capacitive, and hybrid resonators. Feedthrough occurs when an RF electrical signal leaks through the substrate or other parasitic couplings between the drive and sense ports of a resonator instead of undergoing electromechanical conversion. As seen in Figure 9, this was significantly suppressed in hybrid resonators, with more than 30 dB improvement, as compared to those of piezoelectric or capacitive resonators with identical geometry. For comparison, the measured feedthrough level of a CS−5 calibration standard is included. Meanwhile, an increment of the ZnO piezoelectric transducer layer's thickness of a hybrid resonator from 500 nm to 1300 nm further lowers the feedthrough level by more than 50 dB as compared to piezoelectric-only devices, as shown in Figure 8.
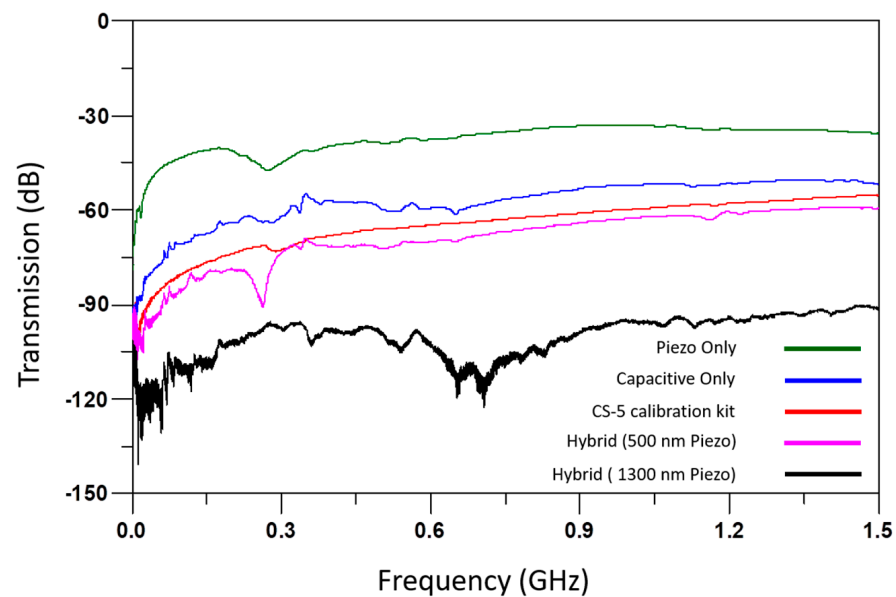

Figure 9. Measured feedthrough levels versus frequency for piezoelectric only, capacitive only, and hybrid resonators with different thin-film piezoelectric transducer thicknesses. The measured feedthrough level of a CS−5 calibration standard is included that exhibits a feedthrough level on par to that of a hybrid device.

The hybrid disk resonators exhibit outstanding performance in frequency characteristics for both the 1st and 4th lateral extensional modes. One hybrid resonator design features two 6 μm-wide side-supporting anchors and narrower capacitive electrodes with smaller capacitive transducer areas, simplifying the gap etching process and lowering the DC actuation voltage needed. However, this design with two anchors leads to a noticeable reduction in acoustic energy influx, negatively impacting the quality factor. Conversely, another design uses a single 10 μm-wide side-supporting anchor with wider capacitive electrodes with a larger capacitive transducer area, as shown in Figure 8b, significantly boosting the quality factor and showing superior frequency responses. As a result, this single-side-supporting anchor hybrid resonator configuration achieves a remarkably loaded *Q*-factor, higher than 28,000 in air, demonstrating the advantages of larger capacitive electrodes in enhancing resonator performance while minimizing the feedthrough. The measured frequency characteristics of these two aforementioned resonator devices are shown in Figures 10 and 11, which depict the measured two-port forward transmission frequency responses for the 1st and 4th contour modes, respectively. Figure 10 presents the measured broadband frequency characteristics of a 125 μm-radius disk resonator with a 5 μm-thick Si device layer operating at its 1st lateral extensional mode. Figure 11 shows the tested broadband frequency characteristics of a 150 μm-radius disk resonator with a 5 μm-thick Si device layer that operates under its 4th lateral extensional mode.
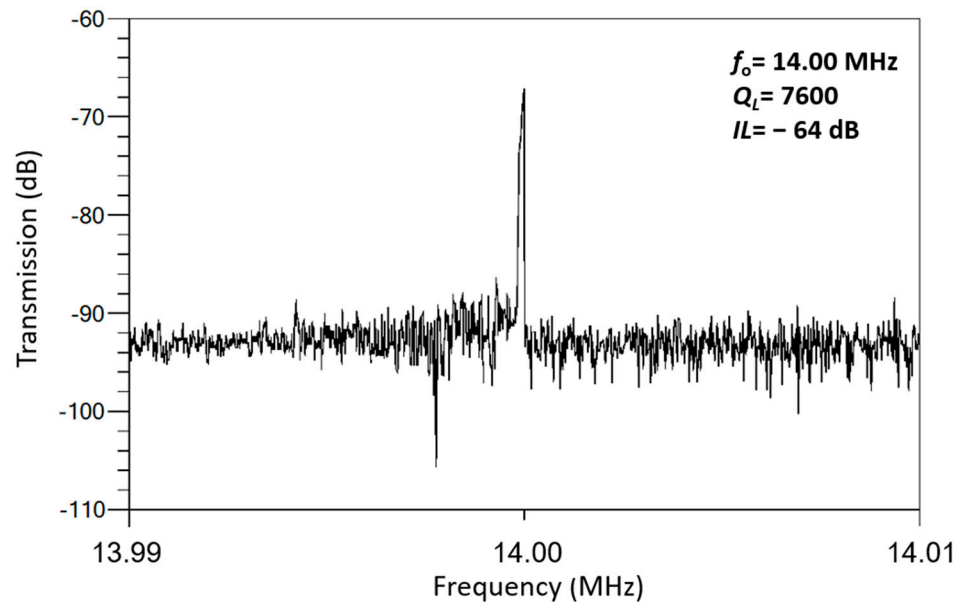
Figure 10. Measured broadband frequency response of a 125 µm−radius hybrid disk resonator with a 5 µm−thick Si device layer operating in its 1st later extensional mode, which is actuated by the fully integrated capacitive transducer through its surrounding electrodes and detected by a piezoelectric transducer via a pair of top electrodes on top of the ZnO piezoelectric layer.

Figure 11. Measured broadband frequency response of a 150 µm−radius hybrid disk resonator, with a 5 µm−thick Si device layer operating in its 4th later extensional mode, which is actuated by the fully integrated capacitive transducer through its surrounding electrodes and detected by a piezoelectric transducer via a pair of top electrodes on top of the ZnO piezoelectric layer.
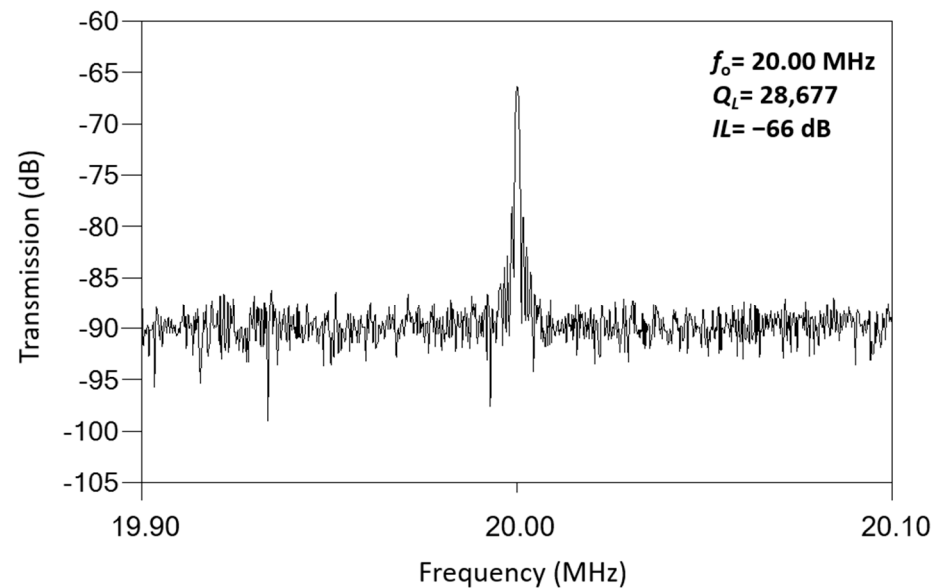
7. Discussion

Hybrid RF MEMS resonators exemplify notable advancements in microelectrome-chanical systems by synergistically integrating capacitive and piezoelectric transduction mechanisms. This innovative design leverages the benefits of both technologies to overcome individual limitations and significantly boost overall device performance, particularly in terms of port-to-port isolation, quality factor, linearity, frequency tuning capabilities, and susceptibility to spurious modes. The hybrid resonator employs a lateral extensional contour-mode device configuration, which is instrumental for allowing the resonator to operate at multiple resonant frequencies on a single chip through lithographically defined

lateral dimensions. This capability is largely attributed to the in-plane lateral dimensions of the shared micromechanical resonator body, allowing for diverse functionality from a single fabrication run. The structural material of choice, low acoustic loss single crystalline silicon, plays a pivotal role in enhancing the linearity and quality factor of the hybrid resonators. This material is renowned for its exceptional acoustic and electrical properties that satisfy the demanding performance needs.

The device's structure includes a resonator body anchored to the substrate via one or two side-supporting anchors designed to minimize acoustic energy dissipation. The strategic positioning of supporting tethers at quasi-nodal points—areas of minimal radial displacement—helps mitigate the loss of acoustic energy through the anchors. This thoughtful placement is critical for preserving the integrity and efficiency of the resonator's model mechanical vibrations, thus maintaining high-quality factor resonances essential for reliable device operation. A key enabling feature of a hybrid resonator's functionality is its layered composition, where a thin film piezoelectric transducer layer (commonly ZnO in this work) is sandwiched between two layers of metal electrodes on top of the resonator body. The top metal layer is intricately patterned to form the drive and sense electrodes, while the bottom layer acts as the ground plane. This setup utilizes the d_{31} piezoelectric coefficients effectively, allowing the resonator to be excited and detected through its contour mode resonances. Meanwhile, the inclusion of electroplated nickel electrodes surrounding the disk-shaped resonator body with a precisely defined capacitive air gap facilitates electrostatic actuation, showcasing the hybrid device's ability to harness multiple transduction mechanisms for enhanced performance.

Table 1 shows the comparison between capacitive, piezoelectric, and hybrid MEMS resonators, highlighting significant differences in their performance metrics including transduction mechanism, operating frequency, bias voltage, gap size, Q-factor and motional impedance. Capacitive resonators, such as the one reported in [28] operating at 96.5 MHz with a *Q*-factor of 3600 and a bias voltage of 7 V, exhibit moderate performance, while another in [29] operates at a much lower frequency of 34 kHz with a high *Q* of 60,000, indicating low energy dissipation with a higher capacitive air gap width of 1000 nm. Piezoelectric resonators, such as the one in [33] operating at 132.94 MHz with a *Q*-factor of 1099, indicate higher energy dissipations as compared to capacitive resonators, whereas another device in [34] operating at a very high frequency (VHF) of 496 MHz with a *Q*-factor of 3800, showing significant performance improvements at higher frequencies. Hybrid resonators, such as the one reported in [37], operate at 101.65 MHz with a *Q*-factor of 14,000, combining both transduction mechanisms for improved performance, while another device in [37] operates at 14.63 MHz with a *Q*-factor of 1952, demonstrating versatility while holding design restrictions. In contrast, this work showcases a notable performance advancement by operating at 20 MHz with an exceptional *Q*-factor of 28,677 while achieving this performance with a lower bias voltage of 12 V and a smaller capacitive air gap width of 84 nm. The higher *Q*-factor and lower bias voltage indicate superior electromechanical coupling coefficient and overall performance, thus making it a standout among reported hybrid resonator technologies. This comparison also underscores the advantages of hybrid resonators, particularly the design presented in this work, which integrates the benefits of both capacitive and piezoelectric mechanisms, achieving high performance with lower energy requirements and advanced fabrication techniques.

The term "hybrid" describes devices that utilize both capacitive and piezoelectric transduction with separate electrodes surrounding the resonator body and physically connected to the piezoelectric layer, respectively. In contrast to reference [37], which utilizes a concave silicon bulk acoustic bar with aluminum nitride as the piezoelectric layer and polysilicon layer, this work adopts a different and more advantageous design. Despite operating at a relatively lower frequency, the resonator reported herein exhibited more than 2-fold higher quality factor while requiring about half of the DC bias voltage as compared to the device in [37]. Additionally, the entire fabrication process has been carried out at a maximum temperature of 400 °C, which is significantly lower than the 1100 °C required

in [37] for the annealing of the doped polysilicon layer and the 850 °C needed to deposit the sacrificial oxide layer. The more recent prior work in hybrid devices [38] primarily employs the capacitive electrode to tune the resonance frequency. While the design has some similarities to this work, employing a capacitive gap, the hybrid resonator in this prior work operates at 14 MHz with a *Q*-factor of 1952 under atmospheric conditions. Moreover, the fabrication approach could only achieve a capacitive air gap of 2.5 μm which is too wide to achieve a desirable electromechanical coupling coefficient. In contrast, this work not only achieves a *Q*-factor that is 14X higher (28,677) but also requires a much lower bias voltage, as illustrated in Table 1. This highlights the superior performance and efficiency of this design. Therefore, the in-house fabrication process used in this work offers significant advantages over other methods, allowing for lower-temperature processes, which is beneficial for integrating devices with CMOS technology. Low-temperature fabrication is crucial as it prevents damage to the metal interconnects or degradation of transistors underneath, ensuring the reliability of the entire integrated microsystem. This resonator achieves a high quality factor and efficient performance with a lower bias voltage, and effectively mitigates parasitic effects, making the design an improved and more efficient solution among all hybrid MEMS resonators. Table 2 presents key fabrication parameter differences of the hybrid resonators reported herein as compared to previous literature.

Table 2. Comparison of fabrication process technologies of among all hybrid resonators equipped with piezoelectric and capacitive transducers.

Reference	Fabrication Method	Piezoelectric Material	Resonator Body Material	Electrode Material Piezoelectric and Capacitive	Resonator Shape and Mode	Features
[37]	AlN-HARPSS	AlN	High-Resistivity Silicon (>1000 Ω-cm)	Molybdenum Polysilicon	Concave bar Width extensional mode	Reaching very high > 1000 °C annealing temperature
[38]	PiezoMUMP	AlN	Doped Silicon	Aluminum Doped Silicon	Disk-shaped Wine-glass mode	Design restrictions from the fabrication methods
This Work	In-house fabrication	ZnO	Low-Resistivity Silicon	Ruthenium Nickel	Lateral extensional Contour mode	High performance at lower temperatures, *Q*-factor > 28,000, parasitic mitigation, lower bias voltage, advanced integration method

The hybrid design's versatility is further strengthened by its ability to support multiple transduction configurations, which satisfy various operational requirements. Each configuration is designed to optimize the resonator's performance by reducing parasitic feedthrough, enhancing port-to-port signal isolation, and improving the suppression of spurious modes. This makes the hybrid MEMS resonator exceptionally suitable for advanced applications in telecommunications, aerospace, and beyond, where precision, efficiency, and reliability are of paramount importance. The ongoing development of these hybrid devices continues to push the boundaries of MEMS technology, promising significant advancements in the field of microfabrication and RF electronic systems.

8. Conclusions

This study has made unique contributions in the field of MEMS by successfully demonstrating the capabilities of a novel hybrid MEMS resonator design that integrates capacitive and piezoelectric transduction mechanisms. This resonator has effectively addressed and overcome some of the fundamental limitations associated with traditional MEMS resonators, particularly in terms of quality factor, insertion loss, and motional impedance, by leveraging the unique advantages of both capacitive and piezoelectric effects within a single device. A notable achievement of this hybrid MEMS resonator is its exceptional ability to minimize parasitic effects that often hinder conventional resonators. The in-

tegration of the two transduction mechanisms is instrumental in significantly reducing parasitic feedthrough, which is a critical barrier in the performance of RF MEMS resonators. By configuring the device to harness the piezoelectric effect for sensing and capacitive (electrostatic) forces for actuation, the resonator demonstrates a substantial decrease in the unwanted signal pathways that typically lead to signal degradation, particularly at higher frequencies. The mitigation of the parasitic effects leads to an improvement in the signal-to-noise ratio, making the hybrid resonator highly effective for precision applications where signal quality and integrity are crucial. Additionally, the resonator shows a remarkable quality factor exceeding 28,000 while operating effectively at frequencies up to 20 MHz. These achievements not only validate the design concept but also highlight the potential of hybrid MEMS resonators to push the frontiers of current RF MEMS technology, offering more reliable and efficient on-chip resonator solutions for advanced telecommunications and electronic warfare systems by combining the advantages of capacitive and piezoelectric mechanisms. This hybrid approach enhances the resonator's performance in terms of quality factor, making it a versatile and robust component for next-generation communication systems. The successful implementation of this new hybrid design marks a pivotal advancement in resonator technology, illustrating a powerful approach to overcoming the traditional trade-offs between performance parameters in MEMS resonators for instance high frequency selectivity filters and high performance oscillators are key components and sub-system modules for communication transceivers. These systems are based on high-Q factor, low parasitic resonators capable of spurious-mode free operation. This provides a solid foundation for the continued evolution of resonator technology, with the hybrid approach offering new pathways for innovation in microfabrication and resonator applications across a wide range of industries, such as telecommunication systems, MEMS resonant mass sensors, and so on, in which they all rely on the vibrating structure to achieve a high-Q factor devices that vibrate at high frequency to satisfy the technological demands of various applications.

Institutional Review Board Statement: Not applicable.

Informed Consent Statement: Not applicable.

Data Availability Statement: The raw data supporting the conclusions of this article will be made available by the authors on request.

Conflicts of Interest: The authors declare no conflict of interest.

References

1. Kurmendra; Kumar, R. A review on RF micro-electro-mechanical-systems (MEMS) switch for radio frequency applications. *Microsyst. Technol.* **2021**, *27*, 2525–2542. [CrossRef]
2. Ozevin, D. MEMS Acoustic Emission Sensors. *Appl. Sci.* **2020**, *10*, 8966. [CrossRef]
3. Pillai, G.; Zope, A.A.; Li, S.-S. Piezoelectric-Based Support Transducer Design to Enable High-Performance Bulk Mode Resonators. *J. Microelectromech. Syst.* **2018**, *28*, 4–13. [CrossRef]
4. Lucyszyn, S. (Ed.) Introduction. In *Advanced RF MEMS*; The Cambridge RF and Microwave Engineering Series; Cambridge University Press: Cambridge, UK, 2010; pp. 1–22. [CrossRef]
5. Yang, R.; Wang, Z.; Lee, J.; Ladhane, K.; Young, D.J.; Feng, P.X.-L. 6H-SiC microdisk torsional resonators in a "smart-cut" technology. *Appl. Phys. Lett.* **2014**, *104*, 091906. [CrossRef]

6. Verma, G.; Mondal, K.; Gupta, A. Si-based MEMS resonant sensor: A review from microfabrication perspective. *Microelectron. J.* **2021**, *118*, 105210. [CrossRef]

7. Liu, W.; Lu, Y.; Chen, Z.; Jia, Q.; Zhao, J.; Niu, B.; Wang, W.; Hao, Y.; Zhu, Y.; Yang, J.; et al. A GHz Silicon-Based Width Extensional Mode MEMS Resonator with Q over 10,000. *Sensors* **2023**, *23*, 3808. [CrossRef]

8. Liu, T.H.; Han, X.; Pastrana, J.; Sepúlveda, N.; Wang, J. Piezoelectric Lateral-Extensional Mode Resonators With Reconfigurable Electrode and Resonance Mode-Switching Behavior Enabled by a VO$_2$ Thin-Film. *IEEE Trans. Ultrason. Ferroelectr. Freq. Control* **2022**, *69*, 2512–2525. [CrossRef]

9. Nilchi, J.N.; Liu, R.; Nguyen, C.T.-C. High Cx/Co 13nm-capacitive-gap transduced disk resonator. In Proceedings of the 2017 IEEE 30th International Conference on Micro Electro Mechanical Systems (MEMS), Las Vegas, NV, USA, 22–26 January 2017; pp. 924–927. [CrossRef]

10. Cai, X.; Wang, Y.; Cao, Y.; Yang, W.; Xia, T.; Li, W. Flexural-Mode Piezoelectric Resonators: Structure, Performance, and Emerging Applications in Physical Sensing Technology, Micropower Systems, and Biomedicine. *Sensors* **2024**, *24*, 3625. [CrossRef]

11. Feng, T.; Yuan, Q.; Yu, D.; Wu, B.; Wang, H. Concepts and Key Technologies of Microelectromechanical Systems Resonators. *Micromachines* **2022**, *13*, 2195. [CrossRef]

12. Kramer, J.; Barrera, O.; Cho, S.; Chulukhadze, V.; Hsu, T.-H.; Lu, R. Experimental Study of Periodically Poled Piezoelectric Film Lithium Niobate Resonator at Cryogenic Temperatures. *arXiv* **2024**, arXiv:2403.09822.

13. Stolt, E.; Braun, W.D.; Gu, L.; Segovia-Fernandez, J.; Chakraborty, S.; Lu, R.; Rivas-Davila, J. Fixed-Frequency Control of Piezoelectric Resonator DC-DC Converters for Spurious Mode Avoidance. *IEEE Open J. Power Electron.* **2021**, *2*, 582–590. [CrossRef]

14. Nguyen, K.; Stolt, E.; Braun, W.; Chulukhadze, V.; Segovia-Fernandez, J.; Chakraborty, S.; Rivas-Davila, J.; Lu, R. Spurious-Free Lithium Niobate Bulk Acoustic Resonator for Piezoelectric Power Conversion. In Proceedings of the 2023 Joint Conference of the European Frequency and Time Forum and IEEE International Frequency Control Symposium (EFTF/IFCS), Toyama, Japan, 15–19 May 2023; pp. 1–4. [CrossRef]

15. Stolt, E.; Braun, W.; Nguyen, K.; Chulukhadze, V.; Lu, R.; Rivas-Davila, J. A Spurious-Free Piezoelectric Resonator Based 3.2 kW DC–DC Converter for EV On-Board Chargers. *IEEE Trans. Power Electron.* **2023**, *39*, 2478–2488. [CrossRef]

16. Pillai, G.; Li, S.-S. Piezoelectric MEMS Resonators: A Review. *IEEE Sens. J.* **2020**, *21*, 12589–12605. [CrossRef]

17. Elnemr, Y.E.; Abu-Libdeh, A.; Raj, G.C.A.; Birjis, Y.; Nazemi, H.; Munirathinam, P.; Emadi, A. Multi-Transduction-Mechanism Technology, an Emerging Approach to Enhance Sensor Performance. *Sensors* **2023**, *23*, 4457. [CrossRef] [PubMed]

18. Zhang, Y.; Bao, J.-F.; Li, X.-Y.; Zhou, X.; Wu, Z.-H.; Zhang, X.-S. Fully-Differential TPoS Resonators Based on Dual Interdigital Electrodes for Feedthrough Suppression. *Micromachines* **2020**, *11*, 119. [CrossRef]

19. Lee, J.-Y.; Seshia, A. Parasitic Feedthrough Cancellation Techniques for Enhanced Electrical Characterization of Electrostatic Microresonators. *Sens. Actuators A Phys.* **2009**, *156*, 36–42. [CrossRef]

20. Xu, Y.; Lee, J.E.-Y. Single-Device and On-Chip Feedthrough Cancellation for Hybrid MEMS Resonators. *IEEE Trans. Ind. Electron.* **2012**, *59*, 4930–4937. [CrossRef]

21. Fan, C.; Wu, Y.; Gu, L.; Wang, Z.; Liu, W.; Cui, F. Automatic Feedthrough Cancellation Methods for MEMS Gyroscopes. *Proc. Inst. Mech. Eng. Part C J. Mech. Eng. Sci.* **2023**, *238*, 5131–5141. [CrossRef]

22. Qiao, Y.; Shi, Z.; Xu, Y.; Wei, X.; Elhady, A.; Abdel-Rahman, E.; Huan, R.; Zhang, W. Frequency unlocking-based MEMS bifurcation sensors. *Microsyst. Nanoeng.* **2023**, *9*, 58. [CrossRef]

23. Lee, H.S.; Chung, J.; Hwang, G.; Jeong, C.K.; Jung, Y.; Kwak, J.; Kang, H.; Byun, M.; Kim, W.D.; Hur, S.; et al. Flexible inorganic piezoelectric acoustic nanosensors for biomimetic artificial hair cells. *Adv. Funct. Mater.* **2015**, *24*, 6914–6921. [CrossRef]

24. Chen, C.-Y.; Li, M.-H.; Li, S.-S. CMOS-MEMS Resonators and Oscillators : A Review. *Sens. Mater.* **2018**, *30*, 733–756.

25. Tu, C.; Lee, J.E.-Y.; Zhang, X.-S. Dissipation Analysis Methods and Q-Enhancement Strategies in Piezoelectric MEMS Laterally Vibrating Resonators: A Review. *Sensors* **2020**, *20*, 4978. [CrossRef] [PubMed]

26. Rivera, I.; Avila, A.; Wang, J. Fourth-Order Contour Mode ZnO-on-SOI Disk Resonators for Mass Sensing Applications. *Actuators* **2015**, *4*, 60–76. [CrossRef]

27. Wang, J.; Ren, Z.; Nguyen, C.-C. 1.156-GHz self-aligned vibrating micromechanical disk resonator. *IEEE Trans. Ultrason. Ferroelectr. Freq. Control.* **2004**, *51*, 1607–1628. [CrossRef] [PubMed]

28. Lee, S.; Demirci, M.U.; Nguyen, C.T.-C. A 10-MHz micromechanical resonator Pierce reference oscillator for communications Digest of Technical Papers. In Proceedings of the 11th International Conference on Solid-State Sensors & Actuators (Transducers'01), Munich, Germany, 10–14 June 2001; pp. 1094–1097.

29. Cioffi, K.R.; Hsu, W.-T. 32 KHz MEMS-based oscillator for low-power applications. In Proceedings of the 2005 IEEE International Frequency Control Symposium and Exposition, Vancouver, BC, Canada, 29–31 August 2005; pp. 551–558. [CrossRef]

30. Kan, X.; Chen, Z.; Yuan, Q.; Wang, F.; Yang, J.; Yang, F. A Novel Multiple-Frequency RF-MEMS Resonator Based on the Whispering Gallery Modes. *IEEE Trans. Electron Devices* **2019**, *66*, 3683–3685. [CrossRef]

31. Zheng, H.-S.; Tsai, C.-P.; Chen, T.-Y.; Li, W.-C. Cmos-Mems Resonators with Sub-100-Nm Transducer Gap Using Stress Engineering. In Proceedings of the 2022 IEEE 35th International Conference on Micro Electro Mechanical Systems Conference (MEMS), Tokyo, Japan, 9–13 January 2022; pp. 13–16. [CrossRef]

32. Chen, Z.; Wang, T.; Jia, Q.; Yang, J.; Yuan, Q.; Zhu, Y.; Yang, F. A Novel Lamé Mode RF-MEMS resonator with high quality factor. *Int. J. Mech. Sci.* **2021**, *204*, 106484. [CrossRef]

33. Zaman, A.; Alsolami, A.; Wei, M.; Rivera, I.; Baghelani, M.; Wang, J. Lateral Extensional Mode Piezoelectric ZnO-on-Nickel RF MEMS Resonators for Back-End-of-Line Integration. *Micromachines* **2023**, *14*, 1089. [CrossRef]

34. Lavasani, H.M.; Abdolvand, R.; Ayazi, F. A 500MHz Low Phase-Noise A1N-on-Silicon Reference Oscillator. In Proceedings of the 2007 IEEE Custom Integrated Circuits Conference, San Jose, CA, USA, 16–19 September 2007; pp. 599–602. [CrossRef]

35. Li, J.; Chen, Z.; Liu, W.; Yang, J.; Zhu, Y.; Yang, F. A novel piezoelectric RF-MEMS resonator with enhanced quality factor. *J. Micromech. Microeng.* **2022**, *32*, 035002. [CrossRef]

36. Deshpande, P.P.; Pande, R.S.; Patrikar, R.M. Fabrication and characterization of zinc oxide piezoelectric MEMS resonator. *Microsyst. Technol.* **2020**, *26*, 415–423. [CrossRef]

37. Samarao, A.K.; Ayazi, F. Combined capacitive and piezoelectric transduction for high performance silicon microresonators. In Proceedings of the 2011 IEEE 24th International Conference on Micro Electro Mechanical Systems, Cancun, Mexico, 23–27 January 2011; pp. 169–172. [CrossRef]

38. Elsayed, M.Y.; Cicek, P.-V.; Nabki, F.; El-Gamal, M.N. Bulk Mode Disk Resonator With Transverse Piezoelectric Actuation and Electrostatic Tuning. *J. Microelectromech. Syst.* **2016**, *25*, 252–261. [CrossRef]

39. Xie, Q.; Nguyen, C.T.-C. 167-MHz AlN Capacitive-Piezoelectric Oscillator. In Proceedings of the 2020 IEEE International Ultrasonics Symposium (IUS), Las Vegas, NV, USA, 7–11 September 2020; pp. 1–4. [CrossRef]

40. Dewdney Montero, J.M. Low Loss VHF and UHF Filters for Wireless Communications Based on Piezoelectrically-Transduced Micromechanical Resonators. Ph.D. Thesis, University of South Florida, Tampa, FL, USA, 2012.